Journal of Biomechanics 126 (2021) 110622

Contents lists available at ScienceDirect

Journal of Biomechanics

journal homepage: www.elsevier.com/locate/jbiomech

The first virtual patient-specific thrombectomy procedure

Giulia Luraghi [a], Sara Bridio [a], Jose Felix Rodriguez Matas [a], Gabriele Dubini [a], Nikki Boodt [b,c,d], Frank J.H. Gijsen [e,f], Aad van der Lugt [b], Behrooz Fereidoonnezhad [g], Kevin M. Moerman [g], Patrick McGarry [g], Praneeta R. Konduri [h,i], Nerea Arrarte Terreros [h,i], Henk A. Marquering [h,i], Charles B.L.M. Majoie [i], Francesco Migliavacca [a,*], on behalf of the INSIST investigators [1]

[a] Laboratory of Biological Structure Mechanics (LaBS), Department of Chemistry, Materials and Chemical Engineering "Giulio Natta", Politecnico di Milano, Milan, Italy
[b] Department of Radiology and Nuclear Medicine, Erasmus MC, University Medical Center Rotterdam, Rotterdam, the Netherlands
[c] Department of Neurology, Erasmus MC, University Medical Center Rotterdam, Rotterdam, the Netherlands
[d] Department of Public Health, Erasmus MC, University Medical Center Rotterdam, Rotterdam, the Netherlands
[e] Department of Biomedical Engineering, Thoraxcenter, Erasmus MC, University Medical Center Rotterdam, Rotterdam, the Netherlands
[f] Department of Biomechanical Engineering, Delft University of Technology, Delft, the Netherlands
[g] School of Engineering, National University of Ireland Galway, Galway, Ireland
[h] Department of Biomedical Engineering and Physics, Amsterdam UMC, location AMC, Amsterdam, the Netherlands
[i] Department of Radiology and Nuclear Medicine, Amsterdam UMC, location AMC, Amsterdam, the Netherlands

ARTICLE INFO

Keywords:
INSIST
Acute ischemic stroke
Stent-retriever
Finite element analysis
In silico

ABSTRACT

Treatment of acute ischemic stroke has been recently improved with the introduction of endovascular mechanical thrombectomy, a minimally invasive procedure able to remove a clot using aspiration devices and/or stent-retrievers. Despite the promising and encouraging results, improvements to the procedure and to the stent design are the focus of the recent efforts. Computational studies can pave the road to these improvements, providing their ability to describe and accurately reproduce a real procedure. A patient with ischemic stroke due to intracranial large vessel occlusion was selected and after the creation of the cerebral vasculature from computed tomography images and a histologic analysis to determine the clot composition, the entire thrombectomy procedure was virtually replicated. As in the real situation, the computational replica showed that two attempts were necessary to remove the clot, as a result of the position of the stent retriever with respect to the clot. Furthermore, the results indicated that clot fragmentation did not occur as the deformations were mainly in a compressive state without the possibility for clot cracks to propagate. The accurate representation of the procedure can be used as an important step for operative optimization planning and future improvements of stent designs.

1. Introduction

Treatment of acute ischemic stroke (AIS) caused by large vessel occlusion has recently been improved with mechanical thrombectomy (MT) approaches as demonstrated by randomized clinical trials (Berkhemer et al., 2015; Campbell et al., 2015; Goyal et al., 2015; Jovin et al., 2015; Lapergue et al., 2017; Saver et al., 2015; Turk et al., 2019). Removal of clots in the cerebral arteries by means of stent-retrievers has emerged as a new way to mitigate the detrimental effects of acute ischemic stroke and facilitate the patient's recovery. Procedural success, defined as removal of the clot and revascularization of the brain, is dependent on the chance to remove the clot in toto with one or more passes. Many investigators have attempted to improve the interaction between thrombectomy devices and thrombus to increase successful revascularization rates (Chueh et al., 2021; Kühn et al., 2020; Ospel et al., 2019).

Computational analyses are increasingly being used to design new devices and to virtually study the capabilities and efficacy of endovascular treatment (Colombo et al., 2020; Kusner et al., 2021; Luraghi et al., 2020; Migliori et al., 2020; Zaccaria et al., 2020). Furthermore, the

* Corresponding author at: Department of Chemistry, Materials and Chemical Engineering 'Giulio Natta', Politecnico di Milano, Piazza L. da Vinci 32, 20133 Milan, Italy.
E-mail address: francesco.migliavacca@polimi.it (F. Migliavacca).
[1] The INSIST investigators are given in the Appendix.

https://doi.org/10.1016/j.jbiomech.2021.110622
Accepted 5 July 2021
Available online 10 July 2021

analysis of radiological images can provide information on cerebral vasculature and thrombus characteristics (Dutra et al., 2019; Mokin et al., 2020). With these ingredients, a patient-specific simulation of the thrombectomy procedure is theoretically feasible, as demonstrated by previous work on bench-top models of cerebral arteries (Giulia Luraghi et al., 2021). Recently, in silico analyses plays an important role in the regulatory process for biomedical devices (Viceconti et al., 2020a) as verification and validation are key factors to prove the credibility of the numerical simulations (Mulugeta et al., 2018).

We aim to show for the first time the capability of the in silico techniques to simulate with accurate details the thrombectomy procedure in a patient-specific case by identifying the causes of procedural success or unsuccess. Based on a previously validated methodology (Luraghi et al, 2021), a model consisting of the intracranial arteries and thrombus is developed from the baseline pre-treatment computed tomography (CT) scans of the patient; the composition of the clot is extracted from histologic analysis, while the stent-retriever is built from data from the manufacturer. The replica of the simulation was guided and supervised by the expert eye of the interventionist neuroradiologist who performed the real procedure.

2. Materials and methods

2.1. Patient

In this study, a 64-year-old male patient from the Amsterdam University Medical Centers -location AMC with acute left arm and leg paralysis due to an occlusion in the right middle cerebral artery with pre-treatment thin-slice non-contrast computed tomography (NCCT) and computed tomography angiography (CTA) scans was analyzed. The endovascular treatment administered to the patient involved two attempts with TREVO XP 4–20 mm stent (Stryker, US) using flow arrest using an 8 French balloon guide catheter, which resulted in complete reperfusion. The clot was detected at the same location before each attempt (Fig. 1a-b). In the first attempt, the stent was placed thoroughly distal to the proximal part of the thrombus (Fig. 1d) while in the second attempt only two-thirds of the stent was placed distal to the proximal part of the thrombus (Fig. 1e). There were no angiographically evident emboli. The final angiography image shows complete recanalization after the second attempt (Fig. 1c).

2.2. Cerebral vasculature model

2.2.1. Image segmentation

To segment the intracranial arteries, the intracranial region was selected from the NCCT image after excluding skull and air using a threshold and region-growing-based algorithm (Fig. 2a), which has been previously validated (Barros et al., 2020). The NCCT image was subsequently automatically registered to the CTA image along with the segmented intracranial region using Elastix software (Klein et al., 2010). A convolutional neural network (CNN)-based intracranial vessel segmentation software named StrokeViewer (NICO.LAB, Amsterdam, The Netherlands) was used to segment the intracranial arteries. In this method, the CTA image was first registered to an in-house brain atlas using Elastix. A patch-based algorithm classified voxels as vessels based on the Hounsfield Units of the surrounding voxels. The CTA image and the segmented vasculature were registered to the original CTA image space to obtain the results in the patient-specific coordinate system. The anterior vasculature was then automatically selected using a mask. A trained observer corrected the segmentation to only include the intracranial arteries on ITK-SNAP software (Yushkevich et al., 2006). iCAFE (© 2016–2018 University of Washington. Used with permission.), a semi-automated software, was used to extract centerlines, local radius, and label arterial segments (Chen et al., 2018). A surface representation of the raw segmentation is shown in Fig. 2b.

The thrombus imaging characteristics consisting of occlusion location and thrombus length were assessed by an experienced neuroradiologist using a previously developed measurement protocol (Dutra et al., 2019). The NCCT and the CTA scans were registered for the intracranial arteries. The decrease of contrast filling observed on the CTA scan and the corresponding presence of the hyperdense artery sign on the NCCT scan allowed the observer to identify the occlusion location. The observer selected three voxels located proximal to the thrombus, within the thrombus, and distal to the thrombus. The length of the thrombus was measured as the distance between the proximal and distal voxels.

2.2.2. Vessel surface mesh creation

The computed vessel centerline data was used to create the vessel wall surface geometry. The raw centerline data may contain non-smooth jumps in the radius, furthermore, the point spacing is not uniform. Therefore, the centerline data was first sampled evenly, based on geodesic cubic Hermite interpolation. Subsequently, the resampled data were smoothed, based on Humphreys-Classes smoothing (Vollmer et al., 1999) in terms of the coordinates and local radius. Next, the vessel surface meshes were derived with the aid of a level-set image (Fig. 2c). This level-set image intensity is based on the ratio between the distance to the nearest centerline point and the radius at this point (Moerman et al., 2021). Hence a single *iso*-surface for the unit-intensity (where the ratio is 1) appropriately defines the vessel geometry (Fig. 2c-2d). The vessel surface meshes were derived using automated methods created using the open-source MATLAB toolbox GIBBON (Moerman, 2018). The final triangulated surface mesh consisted of linear triangles.

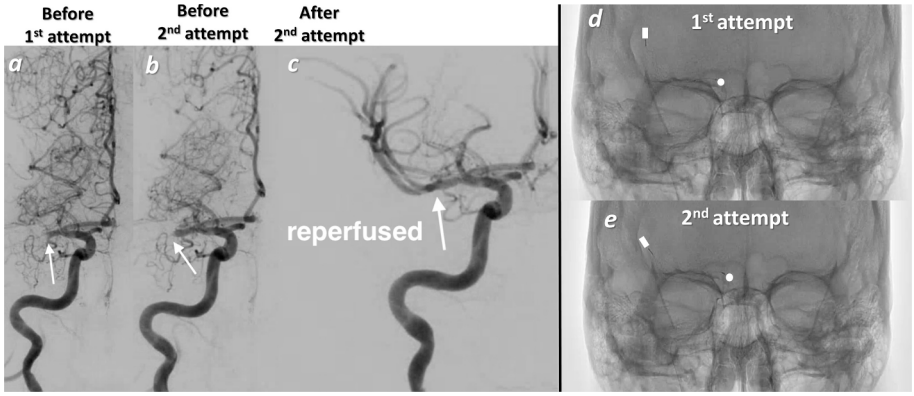

Fig. 1. (a-b) Digital subtraction angiography images in the AP view showing the occlusion of the patient in the right middle cerebral artery before each MT attempt (clot location marked with white arrows) and (c) after the second attempt. (d-e) X-ray images showing the stent deployment in the first and second MT attempt. The stent in the second attempt was positioned more proximal (stent head and tail marked with white points and lines respectively).

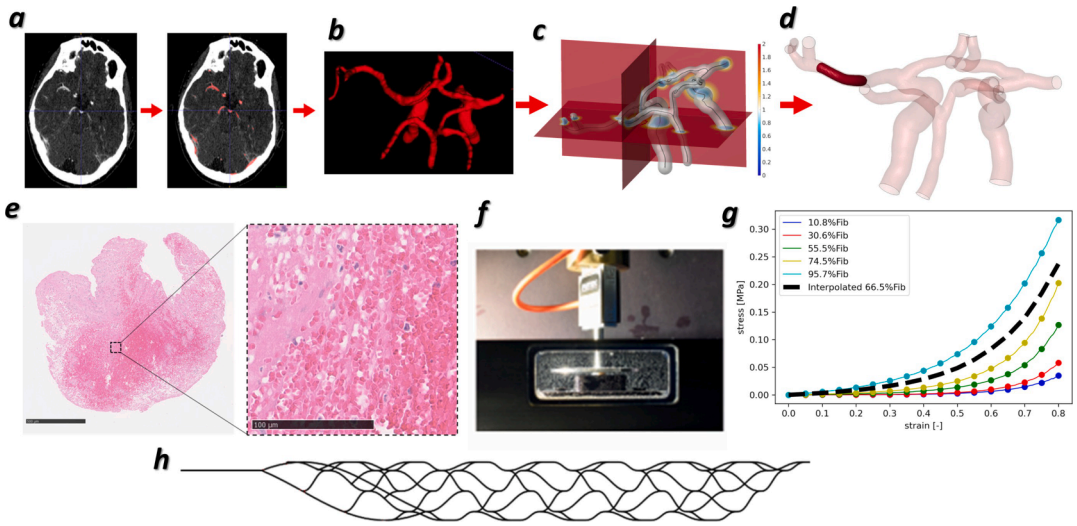

Fig. 2. (a) CT images are segmented to extract the (b) intracranial arteries. (c) Centerlines are processed, and the vessel surface meshes are derived with the aid of a levelset image. (d) Clot location is visible in the transparent representation. (e) Hematoxylin and Eosin histological staining of a clot tested to derive mechanical properties from (f) unconfined compression tests. (g) With increasing fibrin/platelet content, the clot stiffness increases. The stress–strain curve for the patient-specific clot considered in this study (black dotted line) was obtained by interpolating the known curves. (h) Model of the stent-retriever.

2.2.3. Clot composition and mechanical properties

A small prospective study to investigate the relationship between human thrombus composition and mechanical thrombus properties was conducted. Five thrombi with different compositions (in terms of fibrin/platelet content and erythrocyte content) from patients who underwent MT for acute ischemic stroke in the Erasmus University Medical Center in Rotterdam, were mechanically analyzed, directly after MT. All thrombi were retrieved with stent-retrievers. In preparation for the experiments, thrombi were carefully removed from the stent-retriever, after which they were trimmed to a height of one millimeter, such that the resulting sample had a flat top and bottom. The unconfined compression experiments were performed with a custom-built test setup (Boodt et al., 2021), with the test samples submerged in DMEM at body temperature (37 °C) during the experiment. The force tester consisting of an aluminum compression plate, attached to a 2,5N load cell (LSB200 Jr. Miniature S-beam load cell, Futek), which was vertically driven by a linear actuator (EACM4-E15-ZAMK, Oriental motor). The actuator was a stepper motor with a resolution of 0.01 mm, stroke length of 150 mm, and a maximal vertical thrust force of 200 N. The heated basin was controlled by a self-regulating temperature system. Samples were also subjected to 80% compression of their initial height, at a strain rate of 10% per second (Fig. 2f). The applied deformation (strain) of the sample, and the corresponding force exerted by the tissue against the compression plate, were measured. The initial cross-sectional surface areas of the thrombus samples were measured from photographs of the trimmed samples before the experiment, using ImageJ (1.52a, National Institutes of Health, USA). After mechanical testing, thrombus samples were incubated in 4% paraformaldehyde and prepared for histological analysis (Fig. 2e). Thrombi were quantitatively analyzed for fibrin/platelets, erythrocytes, and leukocytes on Hematoxylin and Eosin staining (H&E, HT110216, Sigma-Aldrich, St. Louis, MO, USA), with the use of Orbit Image Analysis (version 3.15, Idorsia Pharmaceuticals Ltd, Allschwil). Stress was obtained by dividing the measured force by the initial cross-sectional surface area of the sample. The mechanical behavior of the tissue was represented in a nominal stress–strain curve. The stress–strain curve for the patient-specific clot considered in this study (with 66.5% of fibrin/platelets) was obtained by interpolating the known curves for which the fibrin/platelet content was known (Fig. 2g).

2.3. Thrombectomy simulation

The details and the verification and validation of the thrombectomy simulation can be found in a previous paper (Giulia Luraghi et al., 2021). Briefly, the stent-retriever model (Fig. 2h) was created using a MATLAB (R2020b, MathWorks, Natick, MA, USA) code. It was discretized with 848 beam elements and modeled with a shape memory alloy to reproduce the Nitinol material. The clot, discretized with 43,960 tetrahedral elements, was modeled with a quasi-hyperelastic foam formulation and a length of 13.7 mm from patient-specific data. The material parameters were obtained by fitting the stress–strain curve representing the patient-specific clot (for the complete clot formulation implemented in the solver see Luraghi et al., 2021). The arterial walls were assumed rigid. The friction coefficients between clot/vessel and clot/stent were 0.3 and 0.1, respectively (Gunning et al., 2018). The simulation of the thrombectomy procedure consisted of *a*) a crimping phase of the stent, *b*) the stent positioning in the location of the clot by following the centerline of the guided catheter, *c*) the stent deployment by unsheathing the microcatheter, *d*) the retrieval of the stent along the catheter centerline with the entrapment of the thrombus defining friction contacts between stent, vessel and clot (Fig. 3). The finite-element models were set up in ANSA Pre Processor (BETA CAE System, Switzerland) and the simulations were performed on a system featuring 40 CPUs (Intel Xeon64) and 256 GB of RAM memory, using the commercial finite-element solver LS-DYNA (ANSYS, USA). Simulation time was approximal 24 h for the entire procedure.

2.4. Fragmentation model

The risk of clot fragmentation during the patient-specific MT was investigated by replicating the deformation of the clot during MT by applying the displacement history of the boundary nodes which are obtained from the thrombectomy simulation; the crack initiation and propagation using the Extended Finite Element Method (XFEM) in Abaqus (Dassualt Systèmes, France) was considered. A damage initiation criterion based on the maximum principal stress (MAXPS) criterion for enriched elements was used. Initial clot crack was not considered before the thrombectomy procedure. The critical MAXPS of 25 kPa has been chosen for crack initiation based on the data reported by Fereidoonnezhad and colleagues for different clot compositions (Fereidoonnezhad et al., 2021). Moreover, the evolution of damage in terms

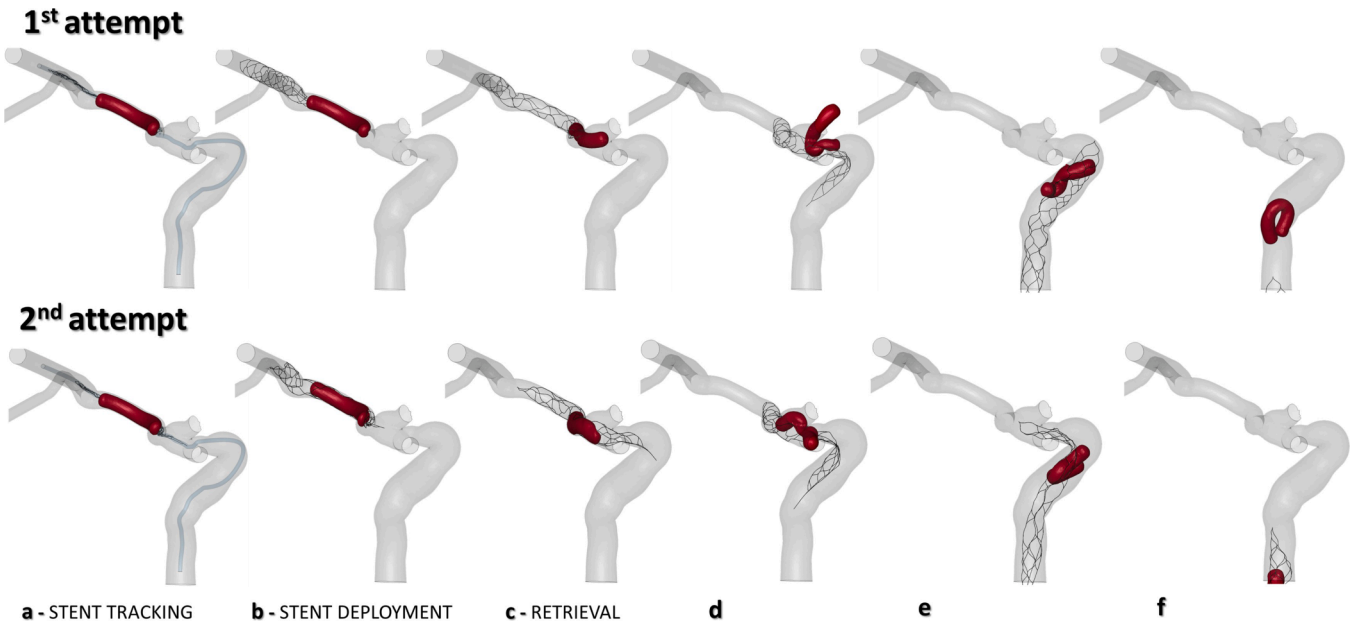

Fig. 3. (a-b) Catheter and stent positions in the first and second attempt during the removal procedure (c-d-e-f). Only the cerebral arteries interested by the procedure are shown. In the first attempt the stent is more distally positioned and the clot escapes from the stent when in the internal carotid artery. In the second attempt the stent is positioned in a way to cover the clot before the stent extraction. In the last image the clot is still entrapped into the stent with a successful outcome.

of the energy required for failure (fracture energy) after the initiation of damage was considered. Based on the experiments of Fereidoonezhad et al. a fracture energy of 0.003 kJ/m^2 is implemented in XFEM simulations. Damage is quantified as a non-dimensional variable D, whereby D = 0 indicates that the initiation criterion has not been reached. Following damage initiation, D increases monotonically as strain energy is released and softening evolves. D = 1 indicates that the critical fracture energy has been exceeded and crack propagation occurs in the XFEM scheme.

3. Results

3.1. Results on extraction

Fig. 3 shows the results of the clot retrieval during the first and the second attempt. The more central stent positioning in the second attempt (Fig. 3a) produced a favorable outcome (Fig. 3f). In fact, the clot was more entrapped inside the stent struts especially in the T-junction areas (Fig. 3d). Furthermore, after the stent expansion in the first attempt (Fig. 3b), the clot was not completely "squeezed" towards the arterial wall; only the distal part of the clot was in contact with the stent indicating that the engagement with the stent struts was weak; an opposite behavior was noticed in the second and successful attempt.

3.2. Results on fragmentation

The clot configuration at the point of maximum tensile stress encountered during thrombectomy is shown in Fig. 4a (during the stent tracking step of the procedure). While several regions of elevated maximum principal stress occur on the surface, the tensile stress is sufficiently high to initiate damage only in one highly localized region, shown in Fig. 4b. A crack is predicted to propagate only ~ 150 μm in the radial direction. As shown in the inset of Fig. 4a, the majority of the cross-section of the thrombus is in a state of compression, therefore

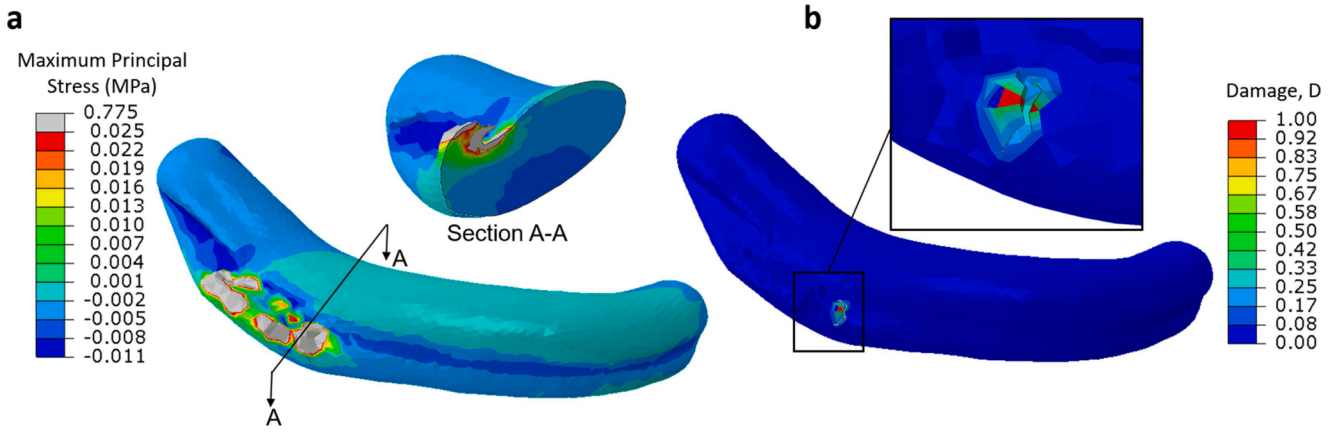

Fig. 4. Prediction of damage initiation and crack propagation during thrombectomy. (a) Distribution of the maximum principal stress in the clot at the location of maximum stress. The results show that the clot is mainly under compressive stress in the radial direction, with localized regions of elevated tensile stress on the surface. (b) Computed damage, D, and XFEM crack propagation in the thrombus. Damage initiation is localized to one region on the thrombus surface and a crack is predicted to propagate only ~150 μm.

crack propagation over a long distance through the thickness of the clot is prevented and clot fragmentation does not occur. This prediction agrees with the clinical observation that the clot remains intact and stays in the same position after the first unsuccessful thrombectomy attempt.

4. Discussion

In silico models are gaining importance in the clinical arena as they can be of help for the interpretation of unknown phenomena, for the prediction of outcome of different interventional techniques, and for testing the performance of different devices. With the improvements in clinical image acquisition, the merging of image post-processing and computational models has become a powerful method to investigate patient-specific details not thinkable a few years ago. The present study is in line with this development and shows for the first time how a detailed thrombectomy procedure with stent-retriever can be virtually replicated starting from the elaboration of CT images analysis, the histology of extracted clots, and sophisticated computer simulations; simulations that necessarily need to be validated (Erdemir et al., 2020; Mulugeta et al., 2018), usually with an in vitro/in silico comparison approach (Giulia Luraghi et al., 2021). In this view, our group recently proposed an applicability analysis to establish the credibility of the thrombectomy simulations (Giulia; Luraghi et al., 2021), following the guidelines provided by the American Society of Mechanical Engineers V&V 40 "Verification and Validation in Computational Modeling of Medical Devices". A proper validation with clinical data dealing with MT is not feasible in the present study because the clot and stent kinematics and clot/stent interaction during the procedure are not detectable by current imaging techniques. Our results were considered reliable and truthful by the interventional neuroradiologist who performed the procedure and confirmed by the literature (van der Marel et al., 2016). Prediction on success of a MT procedure with stent-retriever on a large cohort of patients would be desirable and would certainly strengthen the validity of our results; nonetheless this study represents the first patient-specific attempt in this direction. An important aspect to be considered is that MT is an unplanned procedure. The available clinical data to build an in silico model are limited, if compared to different interventional procedures. Indeed, time is crucial during the MT procedure, the x-ray dosage is minimized with the consequence to reduce the images' availability for modelling purposes, not perfused vessels downstream the occlusion are missing with angiographic images and blood flow rates and pressures are not measured.

Despite the mentioned drawbacks regarding the clinical data not always complete for modelling purposes, the exemplified simulation provided further insight into the reasons for failure (first attempt) and success (second attempt) by revealing thrombus-stent interaction in detail. In particular, the correct stent positioning appears to be an important procedural aspect to be taken into account. The complete stent expansion and clot compression in the second attempt, when compared to the first attempt, revealed the importance of the clot entrapment of the clot within the stent struts as a marker of potential success (Chueh et al., 2021; Kühn et al., 2020; Ospel et al., 2019; Tsumoto et al., 2017). Features like these can be clearly detected and foreseen by a computational simulation, which can help interventionists to optimize their treatment techniques, for example by modeling a different stent retriever. From a different perspective, the capability to run patient-specific simulations with a prediction capability might allow to define and run in silico trials with evident benefits (Konduri et al., 2020; Viceconti et al., 2020b). For this purpose, the complexity of the simulation here proposed would suggest moving future efforts towards the investigation and creation of surrogate models capable of catching the main features of the interventional procedure in a short time. However, we envision that for complex and particular cases the full 3D model as that proposed in this study is a valuable tool for prediction and interpretation.

Despite improvements since the first-generation thrombectomy devices, distal embolism due to clot fragmentation remains a significant challenge for MT procedures (Kühn et al., 2020). In general, all endovascular MT techniques and devices carry a significant risk of thrombus fragmentation and subsequent distal emboli with associated adverse clinical outcomes (Gralla et al., 2006; Kaesmacher et al., 2017; Po Sit, 2009). Fereidoonnezhad et al. have presented the first experimental characterization of the fracture properties of blood clots for a wide range of clot compositions (Fereidoonnezhad et al., 2021). This study attempts also the capability of a computational model to simulate crack initiation and to estimate clot fragmentation. Although the modeled patient did not show clot fragmentation, we demonstrated that also crack initiation and clot fragmentation can be foreseen with a virtual modality. More efforts and validation studies need to be done in this direction.

Lastly, this study is not exempt from limitations. From a modeling point of view, the usage of rigid walls, rigid catheter and unknown patient-specific friction coefficient, together with neglecting the fluid flow from the neighboring communicating arteries, are notable to be mentioned and future studies should be devoted to reduce some of them. Imaging and histological analysis which are necessary for the correct patient-specific modeling present also some limitations. The information acquired from images is limited (e.g. single snapshot in time, 2D images in case of the digital subtraction angiography, etc), while the histological characterization is done post-treatment when the clot is usually already fragmented.

Funding

This project has received funding from the European Union's Horizon 2020 research and innovation program under grant agreement No 777072 and N. Arrarte Terreros also received funding from the AMC medical Research BV, Amsterdam UMC, location AMC, under project No 21937.

Declaration of Competing Interest

The authors declare the following financial interests/personal relationships which may be considered as potential competing interests: [HAM reports co-founder and shareholder of Nico.lab, a company that focuses on the use of artificial intelligence for medical image analysis. CBLMM received funds from the European Commission (related to this project, paid to institution); and from CVON/Dutch Heart Foundation, Stryker, TWIN Foundation, Health Evaluation Program Netherlands (unrelated; all paid to institution). CBLMM is shareholder of Nico.lab, a company that focuses on the use of artificial intelligence for medical imaging analysis]

Acknowledgements

None

Appendix:. INSIST investigators

Charles Majoie[1], Henk Marquering[1,2], Ed van Bavel[2], Alfons Hoekstra[3], Diederik W.J. Dippel[4], Hester L. Lingsma[5], Aad van der Lugt[6], Noor Samuels[4,5,6], Nikki Boodt[4,5,6], Yvo Roos[7], Simon de Meyer[8], Senna Staessens[8], Praneeta Konduri[1,2], Nerea Arrarte Terreros[2],Bastien Chopard[9], Franck Raynaud[9], Remy Petkantchin[9], Vanessa Blanc-Guillemaud[10], Mikhail Panteleev[11,12], Alexey Shibeko[11], Francesco Migliavacca[13], Gabriele Dubini[13], Giulia Luraghi[13], Jose Felix Rodriguez Matas[13], Sara Bridio[13], Patrick Mc Garry[14], Kevin Moerman[14], Behrooz Fereidoonnezhad[14], Michael Gilvarry[15], Ray McCarthy[15], Sharon Duffy[15], Stephen Payne[16], Tamas Jozsa[16], Wahbi El-Bouri[13], Sissy Georgakopoulou[2], Victor Azizi[3], Raymond Padmos[3], Anushree Dwivedi[15]

1 Department of Radiology and Nuclear Medicine, Amsterdam UMC, location AMC, Amsterdam, the Netherlands;

2 Biomedical Engineering and Physics, Amsterdam UMC, location AMC, Amsterdam, the Netherlands;

3 Computational Science Lab, Faculty of Science, Institute for Informatics, University of Amsterdam, Amsterdam, the Netherlands;

4 Department of Neurology, Erasmus MC University Medical Center, PO Box 2040, 3000 CA Rotterdam, the Netherlands;

5 Department of Public Health, Erasmus MC University Medical Center, PO Box 2040, 3000 CA Rotterdam, the Netherlands;

6 Department of Radiology & Nuclear Medicine, Erasmus MC University Medical Center, PO Box 2040, 3000 CA Rotterdam, the Netherlands

7 Department of Neurology, Amsterdam UMC, location AMC, Amsterdam, the Netherlands;

8 Laboratory for Thrombosis Research, KU Leuven Campus Kulak Kortrijk, Kortrijk, Belgium;

9 Computer Science Department, University of Geneva, CUI, 7 route de Drize, 1227 Carouge, Switzerland;

10 Institut de Recherches Internationales Servier, Coubevoie Cedex, France;

11 Center for Theoretical Problems of Physicochemical Pharmacology RAS, Moscow, Russia;

12 Dmitry Rogachev National Research Center of Pediatric Hematology, Oncology and Immunology, Moscow, Russia; Faculty of Physics, Lomonosov Moscow State University, Moscow, Russia;

13 Laboratory of Biological Structure Mechanics (LaBS), Department of Chemistry, Materials and Chemical Engineering “Giulio Natta”, Politecnico di Milano, Milano, Italy.

14 College of Engineering and Informatics, National University of Ireland Galway, Ireland; National Centre for Biomedical Engineering Science, National University of Ireland Galway, Ireland;

15 Cerenovus, Galway Neuro Technology Centre, Galway, Ireland;

16 Institute of Biomedical Engineering, Department of Engineering Science, University of Oxford, Parks Road, Oxford OX1 3PJ, UK.

References

Barros, R.S., Tolhuisen, M.L., Boers, A.M.M., Jansen, I., Ponomareva, E., Dippel, D.W.J., Van Der Lugt, A., Van Oostenbrugge, R.J., Van Zwam, W.H., Berkhemer, O.A., Goyal, M., Demchuk, A.M., Menon, B.K., Mitchell, P., Hill, M.D., Jovin, T.G., Davalos, A., Campbell, B.C.V., Saver, J.L., Roos, Y.B.W.E.M., Muir, K.W., White, P., Bracard, S., Guillemin, F., Olabarriaga, S.D., Majoie, C.B.L.M., Marquering, H.A., 2020. Automatic segmentation of cerebral infarcts in follow-up computed tomography images with convolutional neural networks. J. Neurointerv. Surg. 12, 848–852. https://doi.org/10.1136/neurintsurg-2019-015471.

Berkhemer, O.A., Fransen, P.S.S., Beumer, D., Van den Berg, L.A., Lingsma, H.F., Yoo, A. J., Schonewille, W.J., Vos, J.A., Nederkoorn, P.J., Wermer, M.J.H., van Walderveen, M.A.A., Staals, J., Hofmeijer, J., van Oostayen, J.A., Lycklama à Nijeholt, G.J., Boiten, J., Brouwer, P.A., Emmer, B.J., de Bruijn, S.F., van Dijk, L.C., Kappelle, L.J., Lo, R.H., Van Dijk, E.J., De Vries, J., De Kort, P.L.M., van Rooij, W.J.J., van den Berg, J.S.P., van Hasselt, B.A.A.M., Aerden, L.A.M., Dallinga, R.J., Visser, M.C., Bot, J.C.J., Vroomen, P.C., Eshghi, O., Schreuder, T.H.C.M.L., Heijboer, R.J.J., Keizer, K., Tielbeek, A. V., den Hertog, H.M., Gerrits, D.G., van den Berg-Vos, R.M., Karas, G.B., Steyerberg, E.W., Flach, H.Z., Marquering, H.A., Sprengers, M.E.S., Jenniskens, S.F. M., Beenen, L.F.M., van den Berg, R., Koudstaal, P.J., van Zwam, W.H., Roos, Y.B.W. E.M., van der Lugt, A., van Oostenbrugge, R.J., Majoie, C.B.L.M., Dippel, D.W.J., Investigators, M.C., 2015. A Randomized Trial of Intraarterial Treatment for Acute Ischemic Stroke. N. Engl. J. Med. 372, 11–20. Doi: 10.1056/NEJMoa1411587.

Boodt, N., Snouckaert van Schauburg, P.R.W., Hund, H.M., Fereidoonnezhad, B., McGarry, J.P., Akyildiz, A.C., van Es, A.C.G.M., De Meyer, S.F., Dippel, D.W.J., Lingsma, H.F., van Beusekom, H.M.M., van der Lugt, A., Gijsen, F.J.H., 2021. Mechanical Characterization of Thrombi Retrieved With Endovascular Thrombectomy in Patients With Acute Ischemic Stroke. Stroke. https://doi.org/10.1161/STROKEAHA.120.033527.

Campbell, B.C.V., Mitchell, P.J., Kleinig, T.J., Dewey, H.M., Churilov, L., Yassi, N., Yan, B., Dowling, R.J., Parsons, M.W., Oxley, T.J., Wu, T.Y., Brooks, M., Simpson, M. A., Miteff, F., Levi, C.R., Krause, M., Harrington, T.J., Faulder, K.C., Steinfort, B.S., Priglinger, M., Ang, T., Scroop, R., Barber, P.A., McGuinness, B., Wijeratne, T., Phan, T.G., Chong, W., Chandra, R.V., Bladin, C.F., Badve, M., Rice, H., de Villiers, L., Ma, H., Desmond, P.M., Donnan, G.A., Davis, S.M., 2015. Endovascular Therapy for Ischemic Stroke with Perfusion-Imaging Selection. N. Engl. J. Med. 372, 1009–1018. https://doi.org/10.1056/NEJMoa1414792.

Chen, L., Mossa-Basha, M., Balu, N., Canton, G., Sun, J., Pimentel, K., Hatsukami, T.S., Hwang, J.N., Yuan, C., 2018. Development of a quantitative intracranial vascular features extraction tool on 3D MRA using semiautomated open-curve active contour vessel tracing. Magn. Reson. Med. 79, 3229–3238. https://doi.org/10.1002/mrm.26961.

Chueh, J.Y., Marosfoi, M.G., Anagnostakou, V., Arslanian, R.A., Marks, M.P., Gounis, M. J., 2021. Quantitative Characterization of Recanalization and Distal Emboli with a Novel Thrombectomy Device. Cardiovasc. Intervent. Radiol. 44, 318–324. https://doi.org/10.1007/s00270-020-02683-3.

Colombo, M., Luraghi, G., Cestariolo, L., Ravasi, M., Airoldi, A., Chiastra, C., Pennati, G., 2020. Impact of lower limb movement on the hemodynamics of femoropopliteal arteries: a computational study. Med. Eng. Phys. 81, 105–117. https://doi.org/10.1016/j.medengphy.2020.05.004.

Dutra, B.G., Tolhuisen, M.L., Alves, H.C.B.R., Treurniet, K.M., Kappelhof, M., Yoo, A.J., Jansen, I.G.H., Dippel, D.W.J., van Zwam, W.H., van Oostenbrugge, R.J., da Rocha, A.J., Lingsma, H.F., van der Lugt, A., Roos, Y.B.W.E.M., Marquering, H.A., Majoie, C. B.L.M., MR CLEAN Registry Investigators†, 2019. Thrombus Imaging Characteristics and Outcomes in Acute Ischemic Stroke Patients Undergoing Endovascular Treatment. Stroke 50, 2057–2064. Doi: 10.1161/STROKEAHA.118.024247.

Erdemir, A., Mulugeta, L., Ku, J.P., Drach, A., Horner, M., Morrison, T.M., Peng, G.C.Y., Vadigepalli, R., Lytton, W.W., Myers, J.G., 2020. Credible practice of modeling and simulation in healthcare: Ten rules from a multidisciplinary perspective. J. Transl. Med. https://doi.org/10.1186/s12967-020-02540-4.

Fereidoonnezhad, B., Dwivedi, A., Johnson, S., McCarthy, R., McGarry, P., 2021. Blood clot fracture properties are dependent on red blood cell and fibrin content. Acta Biomater. 127 https://doi.org/10.1016/j.actbio.2021.03.052.

Goyal, M., Demchuk, A.M., Menon, B.K., Eesa, M., Rempel, J.L., Thornton, J., Roy, D., Jovin, T.G., Willinsky, R.A., Sapkota, B.L., Dowlatshahi, D., Frei, D.F., Kamal, N.R., Montanera, W.J., Poppe, A.Y., Ryckborst, K.J., Silver, F.L., Shuaib, A., Tampieri, D., Williams, D., Bang, O.Y., Baxter, B.W., Burns, P.A., Choe, H., Heo, J.-H., Holmstedt, C.A., Jankowitz, B., Kelly, M., Linares, G., Mandzia, J.L., Shankar, J., Sohn, S.-I., Swartz, R.H., Barber, P.A., Coutts, S.B., Smith, E.E., Morrish, W.F., Weill, A., Subramaniam, S., Mitha, A.P., Wong, J.H., Lowerison, M.W., Sajobi, T.T., Hill, M.D., 2015. Randomized Assessment of Rapid Endovascular Treatment of Ischemic Stroke. N. Engl. J. Med. 372, 1019–1030. https://doi.org/10.1056/NEJMoa1414905.

Gralla, J., Schroth, G., Remonda, L., Fleischmann, A., Fandino, J., Slotboom, J., Brekennfeld, C., 2006. A dedicated animal model for mechanical thrombectomy in acute stroke. AJNR Am J Neuroradiol 27, 1357–1361.

Gunning, G.M., McArdle, K., Mirza, M., Duffy, S., Gilvarry, M., Brouwer, P.A., 2018. Clot friction variation with fibrin content; implications for resistance to thrombectomy. J. Neurointerv. Surg. 10, 34–38. https://doi.org/10.1136/neurintsurg-2016-012721.

Jovin, T.G., Chamorro, A., Cobo, E., de Miquel, M.A., Molina, C.A., Rovira, A., San Román, L., Serena, J., Abilleira, S., Ribó, M., Millán, M., Urra, X., Cardona, P., López-Cancio, E., Tomasello, A., Castaño, C., Blasco, J., Aja, L., Dorado, L., Quesada, H., Rubiera, M., Hernandez-Pérez, M., Goyal, M., Demchuk, A.M., von Kummer, R., Gallofré, M., Dávalos, A., 2015. Thrombectomy within 8 Hours after Symptom Onset in Ischemic Stroke. N. Engl. J. Med. 372, 2296–2306. https://doi.org/10.1056/NEJMoa1503780.

Kaesmacher, X.J., Boeckh-Behrens, T., Simon, S., Maegerlein, C., Kleine, J.F., Zimmer, C., Schirmer, L., Poppert, H., Huber, T., 2017. Risk of thrombus fragmentation during endovascular stroke treatment. Am. J. Neuroradiol. 38, 991–998. https://doi.org/10.3174/ajnr.A5105.

Klein, S., Staring, M., Murphy, K., Viergever, M.A., Pluim, J.P.W., 2010. Elastix: A toolbox for intensity-based medical image registration. IEEE Trans. Med. Imaging 29, 196–205. https://doi.org/10.1109/TMI.2009.2035616.

Konduri, P.R., Marquering, H.A., van Bavel, E.E., Hoekstra, A., Majoie, C.B.L.M., 2020. In-Silico Trials for Treatment of Acute Ischemic Stroke. Front. Neurol. 11, 1062. https://doi.org/10.3389/fneur.2020.558125.

Kühn, A.L., Vardar, Z., Kraitem, A., King, R.M., Anagnostakou, V., Puri, A.S., Gounis, M. J., 2020. Biomechanics and hemodynamics of stent-retrievers. J. Cereb. Blood Flow Metab. 40, 2350–2365. https://doi.org/10.1177/0271678X20916002.

Kusner, J., Luraghi, G., Khodaee, F., Rodriguez Matas, J.F., Migliavacca, F., Edelman, E. R., Nezami, F.R., 2021. Understanding TAVR device expansion as it relates to morphology of the bicuspid aortic valve: A simulation study. PLoS One 16, e0251579. https://doi.org/10.1371/journal.pone.0251579.

Lapergue, B., Blanc, R., Gory, B., Labreuche, J., Duhamel, A., Marnat, G., Saleme, S., Costalat, V., Bracard, S., Desal, H., Mazighi, M., Consoli, A., Piotin, M., 2017. Effect of endovascular contact aspiration vs stent retriever on revascularization in patients with acute ischemic stroke and large vessel occlusion: The ASTER randomized clinical trial. JAMA - J. Am. Med. Assoc. 318, 443–452. https://doi.org/10.1001/jama.2017.9644.

Luraghi, Giulia, Bridio, S., Miller, C., Hoekstra, A., Rodríguez Matas, J.F., Migliavacca, F., 2021a. Applicability analysis to evaluate credibility of an In Silico Thrombectomy procedure. J. Biomech. https://doi.org/10.1016/J.JBIOMECH.2021.110631.

Luraghi, G., Matas, J.F.R., Beretta, M., Chiozzi, N., Iannetti, L., Migliavacca, F., 2020. The impact of calcification patterns in transcatheter aortic valve performance: a fluid-structure interaction analysis. Comput. Methods Biomech. Biomed. Engin. 14, 1–9. https://doi.org/10.1080/10255842.2020.1817409.

Luraghi, Giulia, Rodriguez Matas, J.F., Dubini, G., Berti, F., Bridio, S., Duffy, S., Dwivedi, A., McCarthy, R., Fereidoonnezhad, B., McGarry, P., Majoie, C.B.L.M., Migliavacca, F., 2021b. Applicability assessment of a stent-retriever thrombectomy finite-element model. Interface Focus 11, 20190123. https://doi.org/10.1098/rsfs.2019.0123.

Migliori, S., Chiastra, C., Bologna, M., Montin, E., Dubini, G., Genuardi, L., Aurigemma, C., Mainardi, L., Burzotta, F., Migliavacca, F., 2020. Application of an OCT-based 3D reconstruction framework to the hemodynamic assessment of an

ulcerated coronary artery plaque. Med. Eng. Phys. 78, 74–81. https://doi.org/10.1016/j.medengphy.2019.12.006.

Moerman, K.M., 2018. GIBBON: The Geometry and Image-Based Bioengineering add-On. J. Open Source Softw. 3, 506. https://doi.org/10.21105/joss.00506.

Moerman, K.M., Konduri, P.R., Fereidoonnezhad, B., Marquering, H.A., van der Lugt, A., Luraghi, G., Bridio, S., Migliavacca, F., Rodriguez Matas, J.F., McGarry, P., 2021. Development of a Patient-Specific Cerebral Vasculature Fluid-Structure-Interaction Model. J. Biomech. https://doi.org/10.31224/osf.io/qaujs.

Mokin, M., Waqas, M., Chin, F., Rai, H., Senko, J., Sparks, A., Ducharme, R.W., Springer, M., Borlongan, C.V., Levy, E.I., Ionita, C., Siddiqui, A.H., 2020. Semi-automated measurement of vascular tortuosity and its implications for mechanical thrombectomy performance. Neuroradiology Epub ahead. https://doi.org/10.1007/s00234-020-02525-6.

Mulugeta, L., Drach, A., Erdemir, A., Hunt, C.A., Horner, M., Ku, J.P., Myers, J.G., Vadigepalli, R., Lytton, W.W., 2018. Credibility, replicability, and reproducibility in simulation for biomedicine and clinical applications in neuroscience. Front. Neuroinform. 12, 18. https://doi.org/10.3389/fninf.2018.00018.

Ospel, J.M., Volny, O., Jayaraman, M., McTaggart, R., Goyal, M., 2019. Optimizing fast first pass complete reperfusion in acute ischemic stroke–the BADDASS approach (BAlloon guiDe with large bore Distal Access catheter with dual aspiration with Stent-retriever as Standard approach). Expert Rev. Med. Devices 16, 955–963. https://doi.org/10.1080/17434440.2019.1684263.

Po Sit, S., 2009. The penumbra pivotal stroke trial: Safety and effectiveness of a new generation of mechanical devices for clot removal in intracranial large vessel occlusive disease. Stroke 40, 2761–2768. https://doi.org/10.1161/STROKEAHA.108.544957.

Saver, J.L., Goyal, M., Bonafe, A., Diener, H.-C., Levy, E.I., Pereira, V.M., Albers, G.W., Cognard, C., Cohen, D.J., Hacke, W., Jansen, O., Jovin, T.G., Mattle, H.P., Nogueira, R.G., Siddiqui, A.H., Yavagal, D.R., Baxter, B.W., Devlin, T.G., Lopes, D.K., Reddy, V. K., du Mesnil de Rochemont, R., Singer, O.C., Jahan, R., 2015. Stent-Retriever Thrombectomy after Intravenous t-PA vs. t-PA Alone in Stroke. N. Engl. J. Med. 372, 2285–2295. Doi: 10.1056/NEJMoa1415061.

Tsumoto, T., Tsurusaki, Y., Tokunaga, S., 2017. Interaction between the stent strut and thrombus characterized by contrast-enhanced high-resolution cone beam CT during deployment of the Solitaire stent retriever. J. Neurointerv. Surg. 9, 843–848. https://doi.org/10.1136/neurintsurg-2016-012492.

Turk, A.S., Siddiqui, A., Fifi, J.T., De Leacy, R.A., Fiorella, D.J., Gu, E., Levy, E.I., Snyder, K.V., Hanel, R.A., Aghaebrahim, A., Woodward, B.K., Hixson, H.R., Chaudry, M.I., Spiotta, A.M., Rai, A.T., Frei, D., Almandoz, J.E.D., Kelly, M., Arthur, A., Baxter, B., English, J., Linfante, I., Fargen, K.M., Mocco, J., 2019. Aspiration thrombectomy versus stent retriever thrombectomy as first-line approach for large vessel occlusion (COMPASS): a multicentre, randomised, open label, blinded outcome, non-inferiority trial. Lancet 393, 998–1008. https://doi.org/10.1016/S0140-6736(19)30297-1.

van der Marel, K., Chueh, J.-Y., Brooks, O.W., King, R.M., Marosfoi, M.G., Langan, E.T., Carniato, S.L., Gounis, M.J., Nogueira, R.G., Puri, A.S., 2016. Quantitative assessment of device-clot interaction for stent retriever thrombectomy. J. Neurointerv. Surg. 8, 1278–1282. https://doi.org/10.1136/neurintsurg-2015-012209.

Viceconti, M., Juarez, M.A., Curreli, C., Pennisi, M., Russo, G., Pappalardo, F., 2020a. Credibility of in Silico Trial Technologies-A Theoretical Framing. IEEE J. Biomed. Heal. Informatics 24, 4–13. https://doi.org/10.1109/JBHI.2019.2949888.

Viceconti, M., Pappalardo, F., Rodriguez, B., Horner, M., Bischoff, J., Musuamba Tshinanu, F., 2020b. In silico trials: Verification, validation and uncertainty quantification of predictive models used in the regulatory evaluation of biomedical products. Methods 185, 120–127. https://doi.org/10.1016/j.ymeth.2020.01.011.

Vollmer, J., Mencl, R., Müller, H., 1999. Improved laplacian smoothing of noisy surface meshes. Comput. Graph. Forum 18, 131–138. https://doi.org/10.1111/1467-8659.00334.

Yushkevich, P.A., Piven, J., Hazlett, H.C., Smith, R.G., Ho, S., Gee, J.C., Gerig, G., 2006. User-guided 3D active contour segmentation of anatomical structures: Significantly improved efficiency and reliability. Neuroimage 31, 1116–1128. https://doi.org/10.1016/j.neuroimage.2006.01.015.

Zaccaria, A., Danielli, F., Gasparotti, E., Fanni, B.M., Celi, S., Pennati, G., Petrini, L., 2020. Left atrial appendage occlusion device: Development and validation of a finite element model. Med. Eng. Phys. 82, 104–118. https://doi.org/10.1016/j.medengphy.2020.05.019.